Main Manuscript for

Colors of entangled two-photon absorption

Oleg Varnavski[1], Sajal Kumar Giri[3], Tse-Min Chiang[3], Charles J. Zeman IV[3], George C. Schatz[3]*, Theodore Goodson III[1,2*]

[1]Department of Chemistry, [2]Applied Physics, University of Michigan, Ann Arbor, Michigan, 48109.University of Michigan, Ann Arbor, Michigan 481093
[3]Department of Chemistry, Northwestern University, Evanston, Illinois 60208-3113

*George C. Schatz
Email: g-schatz@northwestern.edu

*Theodore Goodson III
Email: tgoodson@umich.edu

Author Contributions: O. V. and T.G. performed the experimental work with the microscope, S.G.,T.C, C.Z.,G.S. developed theoretical model, O.V.,S.G., G.S., and T.G. wrote the manuscript. All authors contributed to the discussions.

Competing Interest Statement: The authors declare no competing financial interests

Classification: Physical Sciences, Physics

Keywords: Quantum, entanglement, two-photon, spectrum

This PDF file includes:

Main Text
Figures 1 to 6

Abstract

Multiphoton absorption of entangled photons offers new ways for obtaining unique information about chemical and biological processes. Measurements with entangled photons may enable sensing biological signatures with high selectivity and at very low light levels to protect against photodamage. In this paper, we present a theoretical and experimental study of the excitation wavelength dependence of the entangled two-photon absorption (ETPA) process in a molecular system, which provides new insights into how entanglement affects molecular spectra. We demonstrate that the ETPA excitation spectrum can be different from that of classical TPA as well as that for one-photon resonant absorption (OPA) with photons of doubled frequency. These results are modeled by assuming the ETPA cross section is governed by a two-photon excited state radiative linewidth rather than by electron-phonon interactions, and this leads to excitation spectra that match the observed results. Further we find that the two-photon allowed states with highest TPA and ETPA intensities have high electronic entanglements, with ETPA especially favoring states with the longest radiative lifetimes. These results provide new concepts for the development of quantum light-based spectroscopy and microscopy that will lead to much higher efficiency of ETPA sensors and novel low intensity detection schemes.

Significance Statement

New insights into the interaction of non-classical entangled light with organic molecules have been provided using a combined experimental/theoretical study of the spectrum for absorbing two entangled photons. This spectrum has been found to be different from that for classical light as well as that for one-photon resonant absorption with photons of doubled frequency. The results show that the most important excited states for both classical and quantum light excitation have high electronic entanglements, and that ETPA additionally favors states with long two photon lifetimes. This provides the opportunity to study states of molecules with non-classical light that have fundamentally different properties than are accessible with classical light.

Main Text

Introduction

Over the past decades quantum entanglement has enabled new directions in developing quantum imaging (1), metrology (2), quantum cryptography (3), and information science (4). Emerging quantum spectroscopy has been demonstrated to be a powerful tool that can extract molecular information not accessible with classical light (5,6). Entangled states of photons provide new control knobs for selective molecular excitation, relaxation, and radiative processes (5-7). Related spectroscopy can be extended to the femtosecond time-resolved domain resulting in an ultrafast tool to probe the dynamics of optical excitations. Strong quantum correlations of entangled photons could circumvent certain Fourier uncertainties and enhance the capabilities of the time-resolved spectroscopy (5,7,8). A very important property of entangled photons as a spectroscopic tool is the linear scaling of nonlinear optical signals such as two photon absorption with the incident light intensity (5,9) as this could enable optical sensing and imaging at extremely low probing power (10-12). Specifically, entangled two photon absorption (ETPA) spectroscopy is a technique that utilizes the quantum nature of light to create a powerful spectroscopic tool (8). In ETPA the molecule is promoted from the ground state to the excited state by simultaneously absorbing two entangled photons. This process drastically differs from classical two-photon absorption due to time and spatial correlation between the two photons, and at low photon flux, the ETPA signal scales linearly rather than quadratically with photon flux (9,13-15). Importantly, the increased bandwidth of the entangled photons does not suppress the two-photon absorption probability due to anticorrelated frequencies of two photons in the pair for the spectrally narrow pump of a spontaneous parametric downconversion (SPDC) source of entangled photons (8). ETPA has attracted considerable attention over the last decades (8,14-17). However, many details of the ETPA absorption mechanism remain unclear; there are still substantial gaps between experimental observations and theoretical modeling (13,14,17-21). Experimentally, it is challenging to clearly distinguish one–photon processes (such as scattering, and hot band absorption) from the linear dependent and relatively weak true ETPA (17,20,22). Various approaches such as using different attenuation schemes affecting photon statistics (21,23), measuring ETPA-excited fluorescence (11,24,25), exploring the spectral width (26) and spatial ETPA dependence (27), as well as HOM-dip detection schemes (28) have been employed to discriminate true ETPA from other contributions. In spite of these efforts there are still substantial deviations in experimentally estimated ETPA cross sections for similar molecules (20,25,29-31) as well as differences between experimental results and theoretical predictions (5,17-19). This makes it difficult to figure out the detailed mechanism of ETPA and its optimal application.

A key issue in providing convincing data that demonstrate ETPA is that the experiments are hard for parametric down-conversion sources, typically involving measurements at a single two-photon energy corresponding to a resonant transition. As a result, variation of the ETPA cross section with excitation energy has not been reported. An action ETPA spectrum that is different from the classical TPA action spectrum would indicate a specific entanglement contribution to the absorption process, which has not been considered by most of the existing theories. Having this information is also essential for separating out competing effects, as hot bands should have a distinct signature related to one-photon absorption (OPA) if these are important, while TPA and ETPA might be expected to have essentially the same action spectrum given that the cross section expressions are very closely related (14,32,33).

From the perspective of theory, an important aspect for ETPA is determining what factors in the molecular electronic structure make the ETPA action spectrum different from that for TPA. One issue in this respect is how the entanglement evolves when the two entangled photons are transformed into a molecular doubly excited state. While there are well-defined selection rules for two-photon excitation that also apply to ETPA, the importance of electronic entanglement in ETPA or in TPA is unknown. However, there are examples where strong entanglement fidelity during two photon excitation has been demonstrated, even in the highly dissipative environment associated with plasmon excitation (34,35). Earlier studies have considered other mechanisms (squeezing and pulse shaping) for controlling the selectivity of electronic excitation in comparison with classical TPA (36,37), but not entanglement.

Another theory issue with ETPA is what is the relevant density of states that needs to be used in Fermi's Golden Rule to determine the ETPA cross section. In the work of Kang et al (19), it was assumed that the density of states of the molecules in ETPA is determined by the radiative lifetime of the two-photon excited state. This result is consistent with modeling that has previously been used in atomic physics (14), although the connection of radiative lifetime and electronic entanglement was not considered in this result. However, the entangled plasmon results just mentioned suggest that the excited electronic states excited by entangled photons can be fundamentally different than in TPA, which is important to applications in spectroscopy and microscopy which utilize ETPA (5,8,11).

In this report, we present a study of the excitation wavelength dependence of the ETPA cross section for the molecule zinc tetraphenyl porphyrin (ZnTPP) which provides new insights into the ETPA mechanism. We find that the ETPA spectrum differs from that for classical two-photon absorption as well as from the linear absorption spectrum for photons of doubled energy (Figure 1). The ETPA spectral results are theoretically interpreted in terms of specific quantum states that can be excited by entangled photons compared to un-entangled photon excitation, and we find that the difference between entangled and un-entangled excited state lifetimes plays the crucial role. We also provide experimental results with variations in signal and idler photon intensities and bandwidths that are designed to test whether the observed signal can be attributed to ETPA or some other process.

Results

In our experiments, the entangled photon pairs were produced by a spontaneous parametric downconversion (SPDC) nonlinear BBO crystal pumped by wavelength-tunable laser (see details in *SI Appendix*). To measure the absorption rate of entangled photon pairs we applied a relatively simple transmission change method for ETPA measurements (15, 39), which can be potentially prone to the one photon linear effects such as scattering or hot band absorption (20, 22). Our previous experiments utilizing a similar SPDC and transmission method showed negligible absorption using a single output beam from SPDC (signal or idler) (39), specific spatial effects (27), and a non-trivial dependence of the measured entangled photon absorption as a function of the entanglement time (26). These findings clearly indicated that correlated photons are the origin of the observed absorption in our configuration. A relatively narrow ETPA spectrum is obtained in the current experiments as well as a drastic drop in ETPA response after spectral selection of a single photon in the pair (see below), which also supports correlated photons as the origin of the observed absorption rate.

We have measured the ETPA rate for the molecule zinc tetraphenyl porphyrin (ZnTPP) of at different wavelengths ranging from 740 nm to 900 nm. The ETPA spectrum was then compared with the classical light TPA and linear absorption spectrum for light at a wavelength half of that used for the TPA experiments. The results are shown as a function of the photon pair energy in Figure 2. The classical TPA spectrum for free base tetraphenyl porphyrin was reproduced from the literature data (40-43). Available data for the classical TPA spectrum of ZnTPP demonstrated a similar wavelength dependence trend with the peak located at wavelength below 380nm (43). It is seen from the data shown in Figure 2 that the ETPA absorption spectrum substantially deviates from that of classical TPA. This surprising result contradicts most of the theoretical descriptions that predict similar shapes for ETPA and classical TPA spectra (14,17,18,32,33). In contrast, the theoretical study of Kang et al (19) proposed that ETPA can be dominated by the final state with the longest radiative lifetime, suggesting a different absorption spectral shape for ETPA and classical TPA. This experimental ETPA action spectrum was not available for the comparison previously. The experimental spectral shift between ETPA and classical TPA obtained in experiment can be roughly estimated as 0.438 eV from the distance between peaks of Gaussian best fits of ETPA and classical TPA as shown in Figure 3. This number will be important in connecting with the theory results.

In the current experiments, we have detected a narrow, resonance-like absorption of the entangled photon pairs at ~820nm with the absorption rate linearly dependent on the input flux. This observation of a narrow absorption line is not consistent with broadband linear (one photon) scattering, indicating minor contribution of this mechanism to the observed absorption spectrum. Another linear effect, which can potentially contribute to the observed signal, is hot band absorption (HBA) (22). HBA can affect the amplitude as well as the spectral shape of the detected absorption. Due to strong Boltzmann factor wavelength dependence, HBA can substantially increase the spectral components towards shorter wavelengths, effectively shifting the observed TPA spectrum to the blue with respect to the true TPA spectrum. In our experiments, we observed the opposite trend with the observed ETPA spectrum being shifted to the red from the classical TPA spectrum. Also, a quantitative analysis of the contribution of the HBA to the absorption rate provided in the SI Appendix shows that the contribution of HBA to the observed absorption is negligibly small under our conditions, being 6-7 orders of magnitude smaller than detected rate. To provide additional proof that the absorption signal is associated with ETPA and not to some other one-photon processes we have introduced an asymmetrical spectral selection of the SPDC output and measured the related ETPA response. For the pump wavelength 770 nm we have compared the ETPA rates recorded with our setup using different bandpass filters F2. The first filter was relatively broad allowing the full SPDC spectrum to reach the sample cell without substantial distortion (Figure 3, filter 1, Newport 10BPF70-750). In this case the measured ETPA rate was ~ 3500 photons/s (Figure 4). The second filter (filter 2, Newport HPM810-80) selects photons having wavelengths shorter than the doubled pump central wavelength (central wavelength of the SPDC spectrum). In this case we have selected only one photon from the pair (idler or signal) rejecting the second frequency-anticorrelated photon in the pair under degenerate phase matching conditions. The ETPA signal dropped dramatically by a factor more than 10 to near the detection limit (300 ± 300 photons/s). The absorption rate as a function of the input flux for the two filtering conditions described above is shown in SI Appendix, Fig. S7. It clearly shows that the observed ETPA rate is associated with the presence of the second frequency anticorrelated photon. When this photon is absent the ETPA rate drops to almost zero indicating that entangled photons are the origin of the observed two-photon absorption signal.

The theory study involves new developments starting from the earlier work of Kang et al (19), where extensions to electronic structure theory were implemented to calculate the TPA and ETPA cross sections for two thiophene dendrimers. In that work, a key difference between these processes arises in the distribution of two-photon excited states that is used in the Fermi Golden Rule expression for the cross section. The density of states determines the lineshape function for absorption, and when evaluated on-resonance for excitation, this function is assumed to be proportional to the lifetime of the excited state that is produced by absorption. For TPA it is found that the effective lifetime associated with this state density is on the order of 10 fs, corresponding to the time scale of electron-phonon dephasing interactions in the doubly excited state, as has been previously established (44). For ETPA, it was argued that the appropriate lifetime is determined by the radiative lifetime of the two-photon state, i.e., electron-phonon interactions do not contribute to the entangled state density, and the resulting lifetimes are in the μs to ms range, as calculated using frequencies and transition moments from electronic structure theory.

The ZnTPP molecule used in the current investigation is assumed to be in its ground electronic state $|g\rangle$ (with energy ε_g) before interacting with light. Two-photon absorption (TPA) results in electronic transitions to an excited state $|f\rangle$ (with energy ε_f) through the intermediate states $|m\rangle$ (with energy ε_m). The TPA cross-section is obtained from the rotationally averaged TPA amplitude $\langle T_{fg}^2\rangle$ (46)

$$\delta_r(\omega) = \frac{8\pi^3\omega^2}{(\hbar c)^2}\langle T_{fg}^2\rangle g_{TPA}(\omega, \varepsilon_f, \Gamma), \tag{1}$$

where ω is the photon frequency, c is the speed of light, and g_{TPA} is the lineshape function that describes spectral broadening of the excitation as introduced phenomenologically. The derivation of Eq. (1) is sketched in the *SI Appendix*, Eqs. S1-S7. We consider degenerate photons for both classical and entangled light i.e., $\omega_1 = \omega_2 = \omega$. Rotational averaging is performed in the molecular coordinate frame to account for ensemble averaging in bulk samples. The rotationally averaged transition amplitude is calculated from the transition moments T_{fg}^{ab} (46)

$$\langle T_{fg}^2\rangle = \frac{1}{30}\sum_{a,b}(FT_{fg}^{aa}\bar{T}_{fg}^{bb} + GT_{fg}^{ab}\bar{T}_{fg}^{ab} + HT_{fg}^{ab}\bar{T}_{fg}^{ba}), \tag{2}$$

where a and b represent cartesian coordinates. F, G, and H are polarization-dependent parameters, F=G=H=2 for parallel polarization and F=G=-1, H=4 for perpendicular polarization. For classical light, we use parallel polarization and for entangled light, we consider photons of perpendicular polarization generated through the type-II spontaneous parametric down-conversion (SPDC) process. $\bar{T}$ stands for the complex conjugate of T. For a CW laser under the dipole approximation, the transition moments are given by

$$T_{fg}^{ab} = \sum_m\left[D_m^{ab}\frac{1}{\Delta_m - \mathrm{i}\kappa_m/2} + D_m^{ba}\frac{1}{\Delta_m - \mathrm{i}\kappa_m/2}\right]. \tag{3}$$

D_m^{ba} is the two-photon dipole matrix element obtained from the molecular dipole components, $D_m^{ba} = \langle f|\hat{\mu}_b|m\rangle\langle m|\hat{\mu}_a|g\rangle$. Detunings are denoted as $\Delta_m = ((\varepsilon_m - \varepsilon_g)/\hbar - \omega)$ with the intermediate state energy ε_m and ground state energy ε_g. For TPA, we use a Lorentzian lineshape function (44)

$$g_{TPA}(\omega, \varepsilon_f, \Gamma) = \frac{1}{\pi}\frac{\Gamma}{(2\omega - (\varepsilon_f - \varepsilon_g)/\hbar)^2 + \Gamma^2}, \tag{4}$$

with the excited state damping factor Γ. g_{TPA} peaks around the two-photon resonance frequency with the height $1/\pi\Gamma$. We select $\hbar\Gamma = 0.1$ eV which corresponds to approximately a 13 fs dephasing time of the excited states.

The entangled two-photon absorption (ETPA) cross-section is expressed as (47)

$$\sigma_e(\omega) = \frac{2\pi}{(\epsilon_0 \hbar c)^2 A_e T_e} \omega^2 \langle \tilde{T}_{fg}^2 \rangle g_{ETPA}(\omega, \varepsilon_f, \tau_f, \Gamma), \tag{5a}$$

with A_e being the entanglement area (which we take to be 10^{-6} cm^2 as in earlier studies (14, 19), ϵ_0 the vacuum permittivity, and T_e the entanglement time (taken to be 63 fs). The lineshape function g_{ETPA} is given by:

$$g_{ETPA}(\omega, \varepsilon_f, \tau_f, \Gamma) = \frac{1}{\pi} \frac{\tau_f \Gamma^2}{\left(2\omega - (\varepsilon_f - \varepsilon_g)/\hbar\right)^2 + \Gamma^2}, \tag{5b}$$

$$\tau_f = \sum_{m<f} \left[\frac{4}{3\hbar} \left(\frac{|\varepsilon_f - \varepsilon_m|}{\hbar c} \right)^3 |\langle f | \hat{\mu} | m \rangle|^2 \right]^{-1}, \tag{5c}$$

where τ_f is the ETPA radiative lifetime of the two-photon electronic excited state $|f\rangle$, which we calculate based on energies and transition moments that are in (5c). The term $\tilde{T}_{fg}$ in Eq. (5a) is given by:

$$\tilde{T}_{fg}^{ab} = \sum_m \left[D_m^{ab} \frac{1 - \exp[-iT_e\Delta_m - T_e\kappa_m/2]}{\Delta_m - i\kappa_m/2} + D_m^{ba} \frac{1 - \exp[-iT_e\Delta_m - T_e\kappa_m/2]}{\Delta_m - i\kappa_m/2} \right], \tag{6}$$

where the D's refer to products of transition moments for the two excitations, Δ_m refers to frequency differences, and the κ_m are damping parameters (19). Note that T_e introduces additional phase factors in the ETPA transition amplitude, which is purely a quantum effect and has no classical analog.

The lineshape expression in Eq. (5b) is based on the work of Kang et al. (19), however with further development that is given in the *SI Appendix*. This shows how the very narrow ETPA lineshape function considered by Kang et al evolves to a broad lineshape g_{ETPA} in (5b) after factoring in the contribution from the broad intermediate state $|m\rangle$ in the entangled two photon absorption process, and with an overall amplitude that comes from the narrow lineshape, leading to the lifetime parameter τ_f in (5b).

Discussion

We have performed all electronic structure calculations with TURBOMOLE for the ZnTPP molecule. The molecular geometry is optimized using the B3LYP hybrid functional and def2-TZVP basis function. The same level of theory is utilized with time-dependent density functional theory (TDDFT) to compute the first 29 excited states required to calculate the two-photon absorption cross-sections. The excited states are indexed from $|1\rangle$ to $|29\rangle$ covering the energy range [2.27, 4.21] eV. Calculated energy levels and transition dipole matrix elements for the first 18 excited states are shown in Figure 5. We calculate the radiative lifetime of all excited states through Eq.5c which are provided in *SI Appendix*, Table S1 along with their corresponding energies. Figures (5a) and (5b) illustrate the partial contributions to the cross-sections from the various two-photon excited states for TPA and ETPA, respectively. There are multiple excited states in the ZnTPP molecule that are two-photon allowed. Among those, we find that state $|16\rangle$ makes the dominant contribution to TPA while the state $|8\rangle$ dominates in ETPA. Higher energy states ($|22\rangle$, $|26\rangle$, and $|28\rangle$) also contribute significantly to TPA, leading to an overall peak intensity at 4.16 eV. By contrast, the ETPA intensity peaks at energy of 3.67 eV due to the combined effect of states $|8\rangle$ and $|11\rangle$. As a result, the ETPA spectrum is red-shifted compared to the TPA spectrum by 0.41 eV (when the subpeaks in TPA are averaged), which is in very good agreement with the experimental shift, 0.44 eV. On the other hand, when compared to the one-photon absorption (OPA) spectrum, the red line in Fig.(5c), both ETPA and TPA spectra are blue-shifted. This qualitatively matches the experimental results in Figure 2, however we note that the calculated energies are all shifted to the blue compared to the measured results by a few tenths of an eV. This is a typical error arising from the use of TDDFT(19) in determining excited state energies and transition moments. Also,the calculations are for gas-phase ZnTPP, so there should be a small solvent red shift that we do not include in the calculations.

Also of significance is that the spectral amplitude (the size of the cross sections) matches well with experiment for both TPA and ETPA. The calculated and measured values of TPA cross-sections are 27 GM and 30 GM, respectively, while the calculated value for ETPA is smaller than experiment by a factor of 10, which is within the precision of the comparison given the uncertainties in excited state energies, transition moments and the entanglement area (19).

Now we discuss Figure 4 in more detail. The transition dipole matrix in Fig. (4b) shows that the ground state $|0\rangle$ is coupled effectively with two nearly degenerate excited states $|3\rangle$ and $|4\rangle$. Therefore, the main OPA peak involves $|0\rangle \rightarrow |3\rangle$ and $|0\rangle \rightarrow |4\rangle$ transitions and for the two-photon transitions, these states ($|3\rangle$ and $|4\rangle$) serve as the important intermediate states. We further note that other high energy excited states (like $|9\rangle$ and $|10\rangle$) participate into the two-photon process as intermediate states but with relatively smaller contributions. TPA populates the state $|16\rangle$ with the maximum intensity due to the large transition moment to this state from the intermediate states and small detuning factors Δ_m associated with this state. There are also large TPA transition amplitudes to higher energy states between [4.1- 4.2] eV ($|22\rangle$, $|26\rangle$, and $|28\rangle$). For ETPA, the same transition moments and detuning factors Δ_m are involved, but the relevance of the different final states varies because of how the cross-section depends on the excited state lifetime τ_f. In this example for the ZnTPP molecule the lifetime is longest for state $|8\rangle$ followed by $|11\rangle$ among the two-photon allowed states (those with non-zero transition moments D_m); see *SI Appendix*, Table S1. As a result, the ETPA spectrum shows the highest peak near these states following the transition paths $|0\rangle \rightarrow |3\rangle/|4\rangle \rightarrow |8\rangle$ and $|0\rangle \rightarrow |3\rangle/|4\rangle \rightarrow |11\rangle$ in addition to the paths $|0\rangle \rightarrow |3\rangle/|4\rangle \rightarrow |16\rangle$ and other transitions that are also accessible by classical light, but are comparatively weak due to the small lifetimes.

Another result from an analysis of the excited states is that the most important ETPA excited states, $|8\rangle$ and $|11\rangle$, are highly entangled, with wavefunctions that are composed of a sum of two configurations with nearly equal weights (see *SI Appendix,* Table S2). The other two-photon excited states, such as those that are dominant in TPA, also involve superpositions of multiple configurations and have Schmidt numbers that are similar to those that dominate in ETPA, as presented in *SI Appendix*, Table S3. Here Schmidt number (a measure of the degree of entanglement that is also known as the collectivity number) has been defined based on natural transition orbital eigenvalues as obtained from TDDFT (48). The dominance of highly entangled two photon excited states in both ETPA and TPA is understandable, as such states involve a coherent sum of single electron-hole excitations such that the transition moment when the second photon is absorbed can be significantly large. For state $|8\rangle$, ETPA is also favored due to the long lifetime associated with this state. This results because the large transition moment associated with two-photon state $|8\rangle$ is for intermediate states $|9\rangle$ and $|10\rangle$, but these are states that are higher in energy than state $|8\rangle$ and thus do not contribute to the lifetime, The other important two-photon states ($|11\rangle$ and $|16\rangle$) have comparatively smaller lifetimes as they are coupled to many lower energy excited states including $|9\rangle$ and $|10\rangle$. Due to large transition moments and small detuning factors Δ_m, state $|16\rangle$ is preferentially excited in TPA, but for ETPA, state $|8\rangle$ dominates because of its significantly longer radiative lifetime.

The theory analysis thus reveals the importance of radiative lifetime in ETPA, which is a property that is favored when there are small energy spacings and transition moments for transitions down from the two photon excited state. Also note that the blue shift of ETPA compared to OPA provides strong evidence that the ETPA signal is different from OPA, otherwise one would see the ETPA peak (assuming the signal and idler photons are both absorbed in one photon transitions) at the same energy as the OPA peak.

We have experimentally shown that the ETPA spectrum can be different from the two-photon absorption spectrum for classical light. In addition, there is a good comparison of these results with calculations where it is assumed that there is an important difference between the densities of states accessible in the two photon excited states in ETPA and TPA as manifested by the excited state lifetimes. Entanglement fidelity can play a role, but the present results show that unentangled photons, i.e., classical light, can efficiently access states with high electronic entanglements via TPA. However it is clear that ETPA provides an opportunity to access excite states of molecules that have fundamentally different properties than with classical light, providing important directions for further quantum light studies.

Materials and Method

In our experiments, the entangled photons were produced by a spontaneous parametric downconversion (SPDC) nonlinear BBO crystal. A wavelength tunable femtosecond laser system SpiritOne -8 (Spectra Physics) was used as the SPDC pump source. The laser system was able to generate the femtosecond pulses (~350 fs duration) with a repetition rate 200 kHz in a broad spectral range covering the visible and NIR. In the current experiments, we tuned the laser wavelength in the range 370 nm – 450 nm to pump SPDC which was based on 1mm thick β-barium borate (BBO) Type II nonlinear crystal (see more details in Materials and Methods of *SI Appendix*). We were able to tune the SPDC output wavelength in the range of 740 nm – 900 nm by using BBO crystals cut for collinear Type II SPDC for 355 nm and 405 nm pump. By adjusting the BBO angle and choosing the output spectral band pass filter (BF2, Figure 6) degenerate photon pairs were produced for each particular pump wavelength. The spectral width of the SPDC output was ~15 nm corresponding to an entanglement time ~63 fs that was measured in previous experiments (16,24,30,49). The pump laser spectral width was in the range 1.7 nm to 2.2 nm (FWHM) depending on the wavelength (*SI Appendix*, Fig. S1).

A dichroic mirror (DM) and a set of band pass filters were used to filter the down converted photons from the pump beam. The entangled photons were focused into a cuvette containing the sample or solvent, and the photon count rate of the transmitted beam was measured using a silicon avalanche photodiode (Perkin Elmer SPCM-AQR-13). A series of variable apertures were used to select the central overlap portion of the SPDC output light cones in a collinear phase-matching arrangement (27) (Fig. S4). The count rate of sample input photon pairs was calibrated vs SPDC pump power. A set of fixed neutral density filters (NF1, Figure 6) and a variable density filter was used to adjust the sample input photon rate. The photon rate transmitted through the sample was measured at each pump power. The difference between the transmitted photon rate for the solvent and for the molecular solution was used to determine the ETPA rate of the sample. The slope of the absorption rate of the sample as a function of input photon rate, along with the sample concentration, cuvette path length (1 cm), and appropriate conversion factors was used to estimate ETPA cross sections for the molecule (Fig. S6). In our experiments, we used solutions of zinc tetraphenyl porphyrin (Millipore Sigma) in toluene of different concentrations 25 μM, 50 μM, 81 μM, and 124 μM (see more details in *SI Appendix*).The ETPA rate was found to be proportional to the concentration.

Acknowledgments

TG.III acknowledges support from the US Air Force Office of Scientific Research in the Biophysics Program via grant FA9550-20-1-0380, from National Science Foundation through Grant 2004076. All authors acknowledge the Department of Energy, Biological and Environmental Research, under grant DE-SC0022118, including cross section computations. SG, TC, CJZ IV and GCS acknowledge NSF Grant CHE-2055565 for entanglement theory work.

References

1. G. B. Lemos, V. Borish, G. D. Cole, S. Ramelow, R. Lapkiewicz, A.Zeilinger, Quantum imaging with undetected photons, *Nature*, **512**, 409–412 (2014).
2. J.P. Dowling, Quantum optical metrology – the lowdown on high –NOON states, *Contemp. Phys.*, **49**, 125-143 (2008).
3. T. Jennewein, C. Simon, G. Weihs, H.Weinfurter, A. Zeilinger, Quantum Cryptography with Entangled Photons, *Phys. Rev. Lett*., **84**, 4729–4732 (2000).
4. M.A. Nielsen, I.L. Chuang, *Quantum computation and quantum information* (Cambridge Univ. Press, Cambridge 2010).
5. K. E. Dorfman; F. Schlawin, S. Mukamel, Nonlinear optical signals and spectroscopy with quantum light, *Rev. Mod. Phys.*, **88**, 045008 (2016).
6. S. Asban, S. Mukamel, Distinguishability and “which pathway” information in multidimensional interferometric spectroscopy with a single entangled photon pair, *Sci. Adv.*, **7**, eabj4566 (2021).
7. F. Schlawin, K.E. Dorfman, B.P. Fingerhut, S. Mukamel, Suppression of population transport and control of exciton distributions by entangled photons, *Nat. Comm.,* **4**, 1782 (2013).
8. F. Schlawin, K. E. Dorfman, S. Mukamel, Entangled two-photon absorption spectroscopy, *Acc. Chem. Res.*, **51**, 2207-2214 (2018).
9. J. Javanainen, P.L. Gould, Linear intensity dependence of a two-photon transition rate, *Phys. Rev. A*, **41**, 5088-5091 (1990).
10. T. B. Pittman, Y. Shih, D. Strekalov, A.V Sergienko, Optical imaging by means of two-photon quantum entanglement, *Phys. Rev. A*, **52**, 3429-3432 (1995).
11. O. Varnavski, T. Goodson, Two-photon fluorescence microscopy at extremely low excitation intensity: the power of quantum correlations, *J. Am. Chem. Soc.*, **142**, 12966-12975 (2020).
12. O. Varnavski, C. Gunthardt, A. Rehman, G.D. Luker, T. Goodson III, Quantum light-enhanced two-photon imaging of breast cancer cells, *J. Phys. Chem. Lett.*, **13**, 2772−2781 (2022).
13. N. Ph. Georgiades, E.S. Polzik, K. Edamatsu, H. J. Kimble, A. S. Parkins, Nonclassical excitation for atoms in a squeezed vacuum, *Phys. Rev. Lett.*, **75,** 3426-3429 (1995).
14. H.B. Fei, B.M. Jost, S. Popescu, B.E.A. Saleh, M.C. Teich, Entanglement-induced two-photon transparency, *Phys. Rev. Lett.*, **78**, 1679-1682 (1997).
15. D.I. Lee, T. Goodson, Entangled photon absorption in an organic porphyrin dendrimer, *J. Phys. Chem. B*, **110**, 25582-25585 (2006).
16. A. Eshun, O. Varnavski, J.P. Villabona-Monsalve, R.K. Burdick, T. Goodson III, Entangled photon spectroscopy, *Acc. Chem. Res*., **55**, 991−1003 (2022).

17. M.G. Raymer, T. Landes, A.H. Marcus, Entangled two-photon absorption by atoms and molecules: A quantum optics tutorial, *J. Chem. Phys.*, **155**, 081501 (2021).
18. T. Landers, M.G. Raymer, M. Allgaier, S. Mercouche, B. Smith, A.H. Marcus, Quantifying the enhancement of two-photon absorption due to spectral-temporal entanglement, *Opt. Express*, **29**, 20022-20033 (2021).
19. G. Kang, K.N. Avanaki, M.A. Mosquera, R.K. Burdick, J.P. Villabona-Monsalve, T. Goodson III, G. C. Schatz, Efficient modeling of organic chromophores for entangled two-photon absorption, *J. Am. Chem. Soc.*, **142**, 10446-10458 (2020).
20. K.M. Parzuchowski , A. Mikhaylov, M.D. Mazurek, R.N. Wilson, D.J. Lum , T. Gerrits,; C.H. Camp Jr., M.J. Stevens , R. Jimenez, Setting bounds on entangled two-photon absorption cross sections in common fluorophores, *Phys. Rev. Applied*., **15**, 044012 (2021).
21. D. Tabakaev, A. Djorovi´c, L. La Volpe, G. Gaulier, S. Ghosh, L. Bonacina, J.-P. Wolf, H. Zbinden, R.T. Thew, Spatial properties of entangled two-photon absorption, Spatial Properties of Entangled Two-Photon Absorption, *Phys. Rev. Lett.* **129**, 183601 (2022).
22. A. Mikhaylov, R.N. Wilson, K. M. Parzuchowski, M.D. Mazurek, C.H. Camp Jr, M.J. Stevens, R. Jimenez, Hot-band absorption can mimic entangled two-photon absorption, **13**, 1489-1493 (2022).
23. B. Dayan, A. Pe'er, A.A. Fliesem, Y. Silberberg, Nonlinear interactions with an ultrahigh flux of broadband entangled photons, *Phys. Rev. Lett.*, **94**, 043602 (2005).
24. O. Varnavski, B. Pinsky, T. Goodson III, Entangled photon excited fluorescence in organic materials: An ultrafast coincidence detector, *J. Phys. Chem. Lett*., **8**, 388-393 (2017).
25. D. Tabakaev, M. Montagnese, G. Haack, L. Bonacina, H. Zbinden, R. T. Thew, Energy-time entangled two-photon molecular absorption, *Phys. Rev. A*, **103**, 033701 (2021).
26. R.K. Burdick, G.C. Schatz, T. Goodson III, Enhancing entangled two-photon absorption for picosecond quantum spectroscopy *J. Am. Chem. Soc.*, **143**, 16930-16934 (2021).
27. A.R. Guzman, M.R. Harpham, Ö. Süzer, M.M. Haley, T.G. Goodson III, Spatial control of entangled two-photon absorption with organic chromophores *J. Am. Chem. Soc*., **132**, 7840-7841 (2010).
28. F. Triana-Arango, G. Ramos-Ortiz, R. Ramirez-Alarcon, Entangled two-photon absorption detection through a Hong-Ou-Mandel interferometer, *arXiv:2202.05985v1 [quant-ph] 12 Feb* 2022
29. T. Landes, M. Allgaier, S. Merkouche, B.J. Smith, M.H. Marcus, M.G. Raymer, Experimental feasibility of molecular two-photon absorption with isolated time-frequency-entangled photon pairs, *Phys. Rev. Res*., **3**, 033154 (2021).
30. J.P. Villabona-Monsalve, R.K. Burdick, T. Goodson III, Measurements of entangled two-photon absorption in organic molecules with CW-pumped type-I spontaneous parametric down-conversion, *J. Phys. Chem. C*, **124**, 24526-24532 (2020).
31. J. P. Villabona-Monsalve, O. Caldero, M. N. Portela, A.Valencia, Entangled two photon absorption cross section on the 808 nm region for the common dyes zinc tetraphenylporphyrin and rhodamine B, *J. Phys. Chem. A*, **121**, 7869–7875 (2017).
32. R. de J. Leon-Montiel, J. Svozilık, L.J. Salazar-Serrano, J.P. Torres, Role of the spectral shape of quantum correlations in two-photon virtual-state spectroscopy, *New J. Phys*., **15**, 053023 (2013).
33. B. Dayan, Theory of two-photon interactions with broadband down-converted light and entangled photons *Phys. Rev. A.*, **76**, 043813 (2007).

34. X.-H. Jiang, P. Chen, K.-Y. Qian, Z.-Z. Chen, S.-Q. Xu,Y.-B. Xie, S.-N. Zhu, X.-S. Ma, Quantum teleportation mediated by surface plasmon polariton, *Sci. Rep.*, **10,** 11503 (2020).
35. F. Dieleman, M. S. Tame, Y. Sonnefraud, M. S. Kim, S. A. Maier, Experimental Verification of Entanglement Generated in a Plasmonic System. *Nano Lett.* **17**, 7455−7461 (2017).
36. H. Oka, Efficient selective two-photon excitation by tailored quantum –correlated photons, *Phys. Rev. A* **81,** 063819 (2010).
37. S.K. Giri, G.C. Schatz, Manipulating Two-Photon Absorption of Molecules through Efficient Optimization of Entangled Light *J. Phys. Chem. Lett.* **13,** 1014010146 (2022).
38. L. Upton, M. Harpham, O.Suzer, M. Richter, S. Mukamel, T. Goodson, Optically excited entangled states in organic molecules illuminate the dark, *J. Phys. Chem. Lett.***, 4***,* 2046-2052 (2013).
39. M.R. Harpham, O. Suzer, C.-Q. Ma, P. Bauerle, T. Goodson, Thiophene dendrimers as entangled photon sensor materials, *J. Am. Chem. Soc.***, 131**, 973-979 **(**2009).
40. N.S. Makarov, M. Drobizhev, A. Rebane, Two-photon absorption standards in the 550-1600 nm excitation wavelength range. *Opt. Express* **2008,** *16*, 4029-4047.
41. A. Karotki, M. Drobizhev, M. Kruk, C. Spangler, E. Nickel, N. Mamardashvili, A. Rebane, Enhancement of two-photon absorption in tetrapyrrolic compounds, *J. Opt. Soc. Am. B***, 20**, 321-332 (2003).
42. M. Kruk, A. Karotki, M. Drobizhev, V. Kuzmitsky, V. Gael, A. Rebane, Two-photon absorption of tetraphhenylporphyrin free base. *J. Luminescence***, 105***,* 45-55 (2003).
43. D. Yao, L. Shi, Z. Sun, M. Blanchard-Desce, O. Mongin, F. Paul, C.O. Paul-Roth, New fluorescent tetraphenylporphyrin-based dendrimers with alkene-linked fluorenyl antennae designed for oxygen sensirtization, *C.R. Chemie***, 24***,* 57-70 (2021).
44. M.T.P. Beerepoot, D.H. Friese, N.H. List, J. Kongsted, K. Ruud, Benchmarking two-photon absorption cross sections: performance of CC2 and CAM-B3LYP, *Phys. Chem. Chem. Phys.*, **17**, 19306-19314 **(**2015).
45. W.L. Peticolas, Multiphoton Spectroscopy, *Ann. Rev. Phys. Chem.*, **18**, 233-260 (1967).
46. P.R. Monson, W.M. McClain, Polarization dependence of the two-photon absorption of tumbling molecules with application to liquid 1-chloronaphthalene and benzene, *J. Chem. Phys.,* **53**, 29-37 **(**1970).
47. J. Perina, Jr., B. E. A. Saleh, M. C. Teich, Multiphoton absorption cross section and virtual-state spectroscopy for the entangled n-photon state, *Phys. Rev.* A **57**, 3972-3986 (1998).
48. F. Plasser, Entanglement entropy of electronic excitations, *J. Chem. Phys.* **144**, 194107 (2016).
49. A. Eshun, B. Gu, O. Varnavski, S. Asban, K.E. Dorfman, S. Mukamel, T. Goodson, **III**, Investigations of molecular optical properties using quantum light and Hong−Ou−Mandel interferometry, *J. Am. Chem. Soc.***, 143,** 9070−9081 (2021).

Figure Captions

Figure 1. Schematic representation of the entangled two-photon absorption (ETPA) peak with respect to the absorption peak position for classical two-photon absorption (TPA) and for one-photon resonant absorption (OPA).

Figure 2. Entangled two photon absorption spectrum of ZnTPP (filled blue hexagons), classical light two-photon absorption spectrum of TPP (open red circles) (41-44). Blue solid line is the best fit of the ETPA spectrum using two Gaussians, Solid red line is the best fit for classical TPA data using Gaussian. The top of the Gaussian best fit for classical TPA is shown in the energy area 3.37-3.6 eV (re-scaled by factor 0.62). Solid green line is the linear absorption spectrum of ZnTPP.

Figure 3. Transmission of the band pass filters used in the experiments with spectral selection of the SPDC output. Spectrum of frequency entangled photons generated by SPDC is also shown.

Figure 4. (a) Excited state energies (from black to yellow energy increases) and (b) transition dipole matrix for the first 18 excited states. Important states for TPA and ETPA are labeled in (a). States $|3\rangle$ and $|4\rangle$ serve as important intermediate states as there are large transition moments to these states from the ground state $|0\rangle$. Transitions to these intermediate states are shown by green arrows in (a). States $|13\rangle$ and $|16\rangle$ are important for TPA with significant transition moments from these intermediate states. However, state $|8\rangle$ and $|11\rangle$ become crucial in ETPA due to their long radiative lifetimes τ_f.

Figure 5.TPA and ETPA cross-sections as a function of photon frequency. Partial (a) TPA and (b) ETPA cross-sections for the first 29 excited states. The state energy increases from black to yellow lines (see legend). (c) TPA (red) and ETPA (blue) cross-sections. The peak position of the OPA spectrum (green) is compared with TPA and ETPA spectra. Here the damping parameter in Eqs. 1 and 6 is assumed to be $\hbar\kappa_m$=0.1 eV for all intermediate states.

Figure 6. Setup optical diagram. Interference filters (BF1) separate the pump light from a weak residual light with wavelengths other than the main pump produced in a complex optical parametric amplifier system. A dichroic beam splitter DM that is not transparent for the pump directs pump light to the power reference photodetector (PD). A set of neutral filters (NF1) accompanied by the linear variable filter are used to precisely adjust the SPDC pump power. A band pass filter (BF2) is used to filter out the residual pump light.

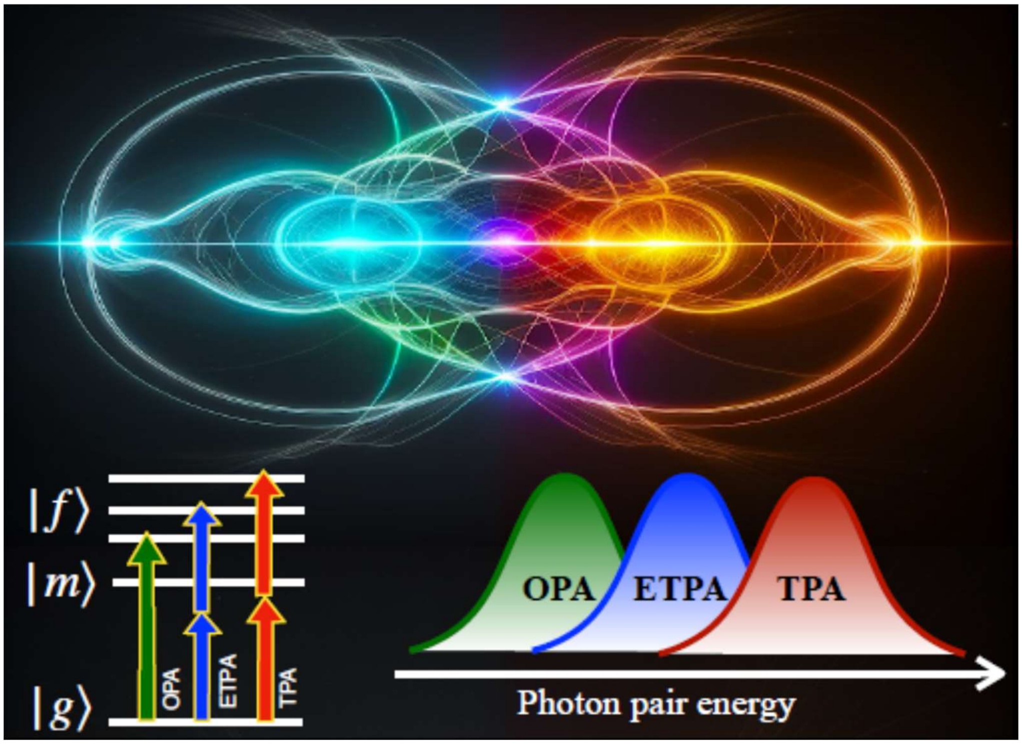
$|f\rangle$
$|m\rangle$
$|g\rangle$
OPA
ETPA
TPA
OPA
ETPA
TPA
Photon pair energy

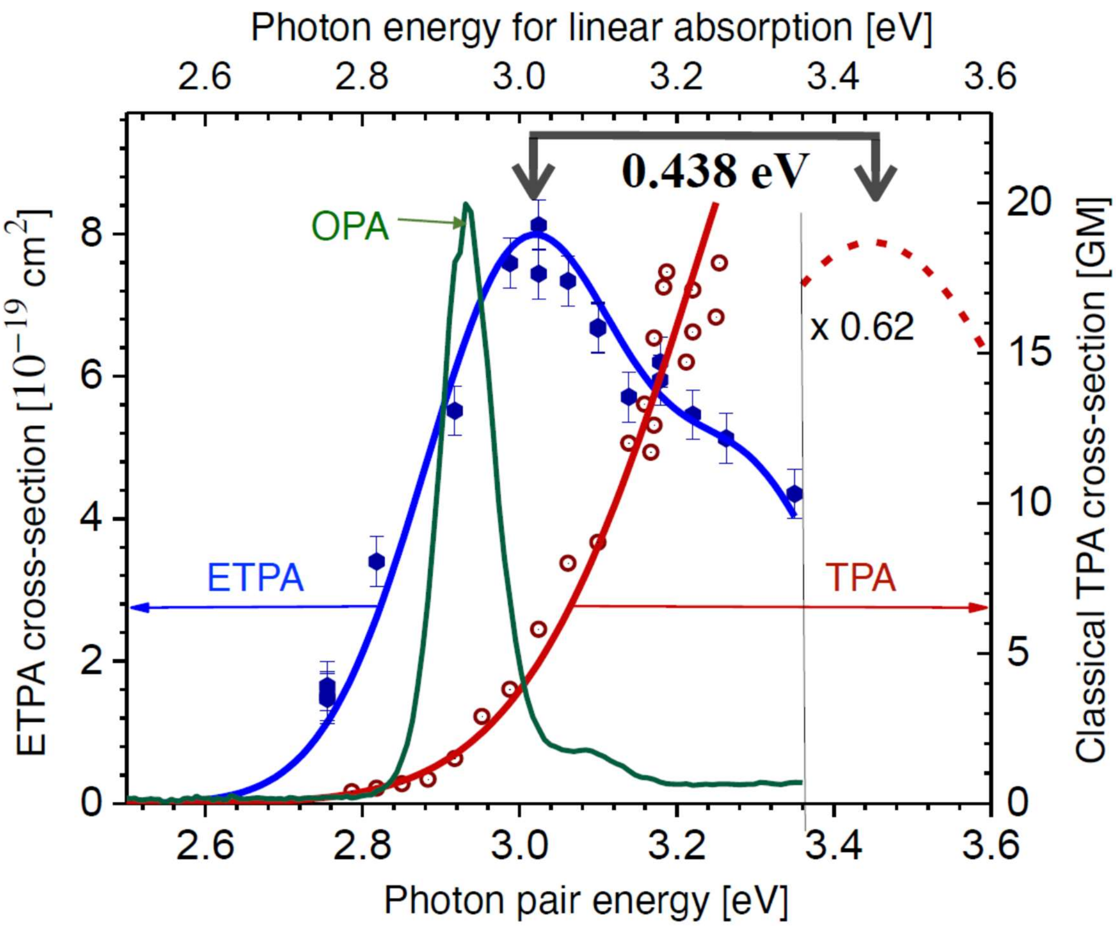
Photon energy for linear absorption [eV]
2.6
2.8
3.0
3.2
3.4
3.6
0.438 eV
OPA
x 0.62
ETPA
TPA
ETPA cross-section [10^{-19} cm^2]
Classical TPA cross-section [GM]
0
2
4
6
8
0
5
10
15
20
Photon pair energy [eV]

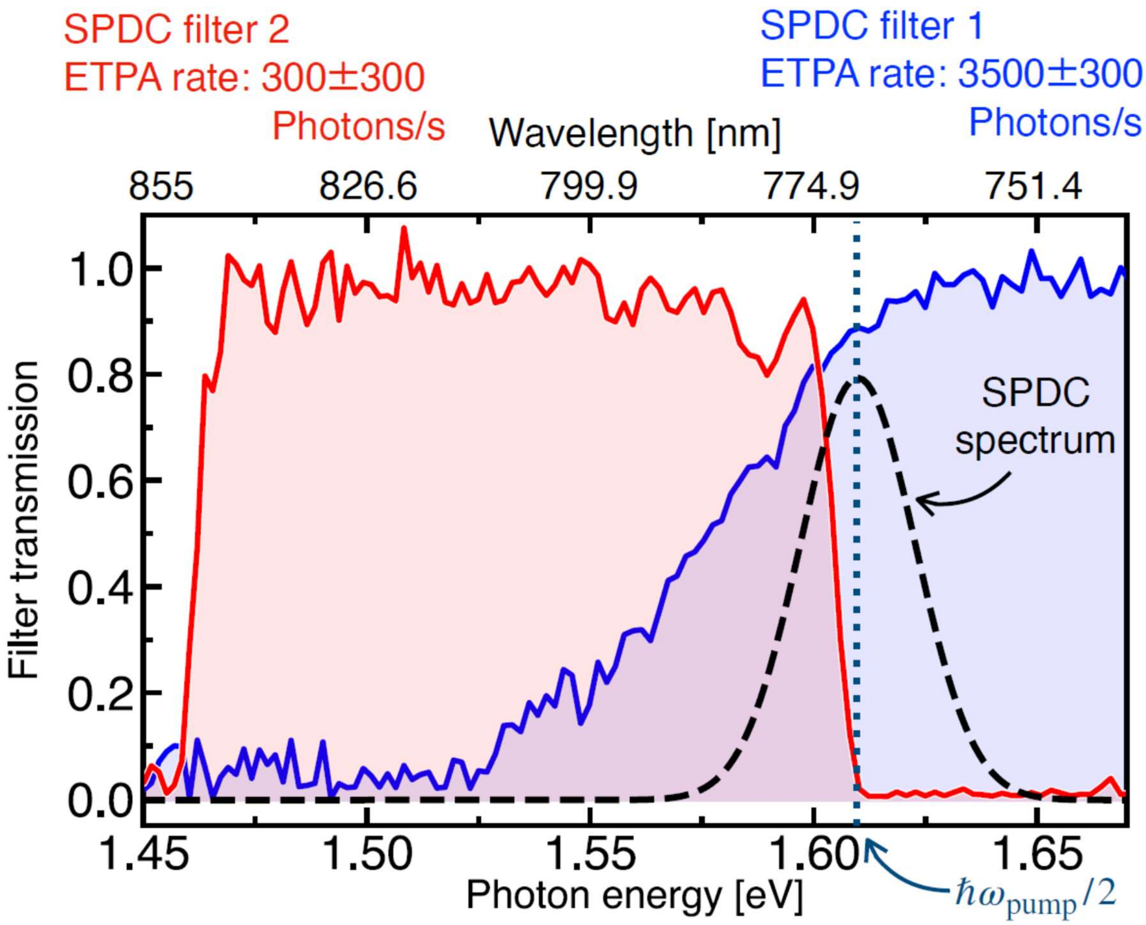

SPDC filter 2
ETPA rate: 300±300
Photons/s
SPDC filter 1
ETPA rate: 3500±300
Photons/s
Wavelength [nm]
855
826.6
799.9
774.9
751.4
Filter transmission
1.0
0.8
0.6
0.4
0.2
0.0
SPDC
spectrum
1.45
1.50
1.55
1.60
1.65
Photon energy [eV]
$\hbar\omega_{\mathrm{pump}}/2$

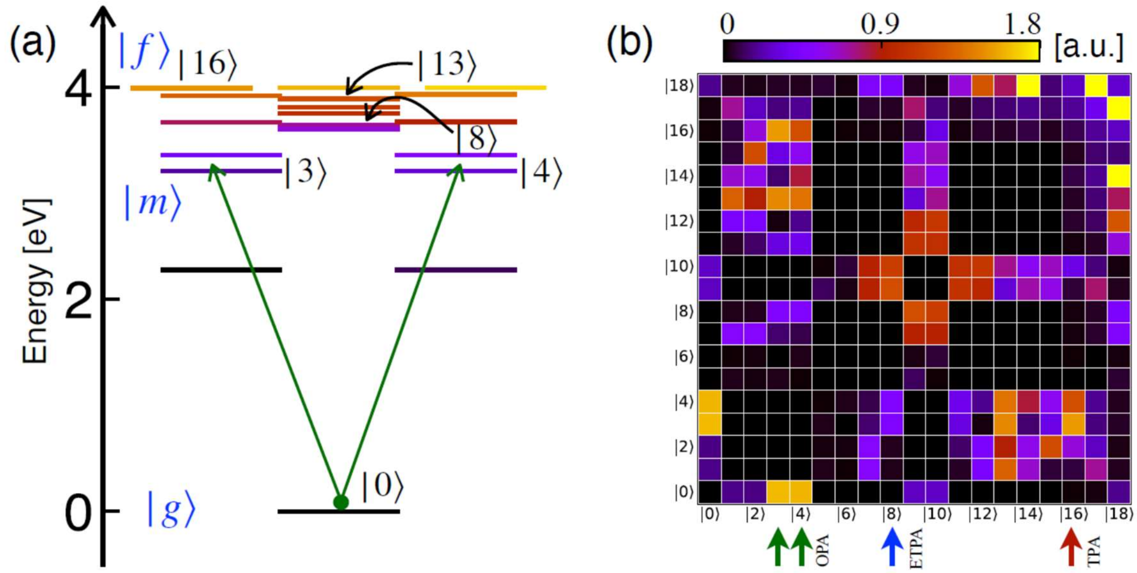

(a)
(b)
Energy [eV]
0
2
4
|f⟩
|16⟩
|13⟩
|8⟩
|3⟩
|4⟩
|m⟩
|0⟩
|g⟩
0
0.9
1.8
[a.u.]
|18⟩
|16⟩
|14⟩
|12⟩
|10⟩
|8⟩
|6⟩
|4⟩
|2⟩
|0⟩
|0⟩
|2⟩
|4⟩
|6⟩
|8⟩
|10⟩
|12⟩
|14⟩
|16⟩
|18⟩
OPA
ETPA
TPA

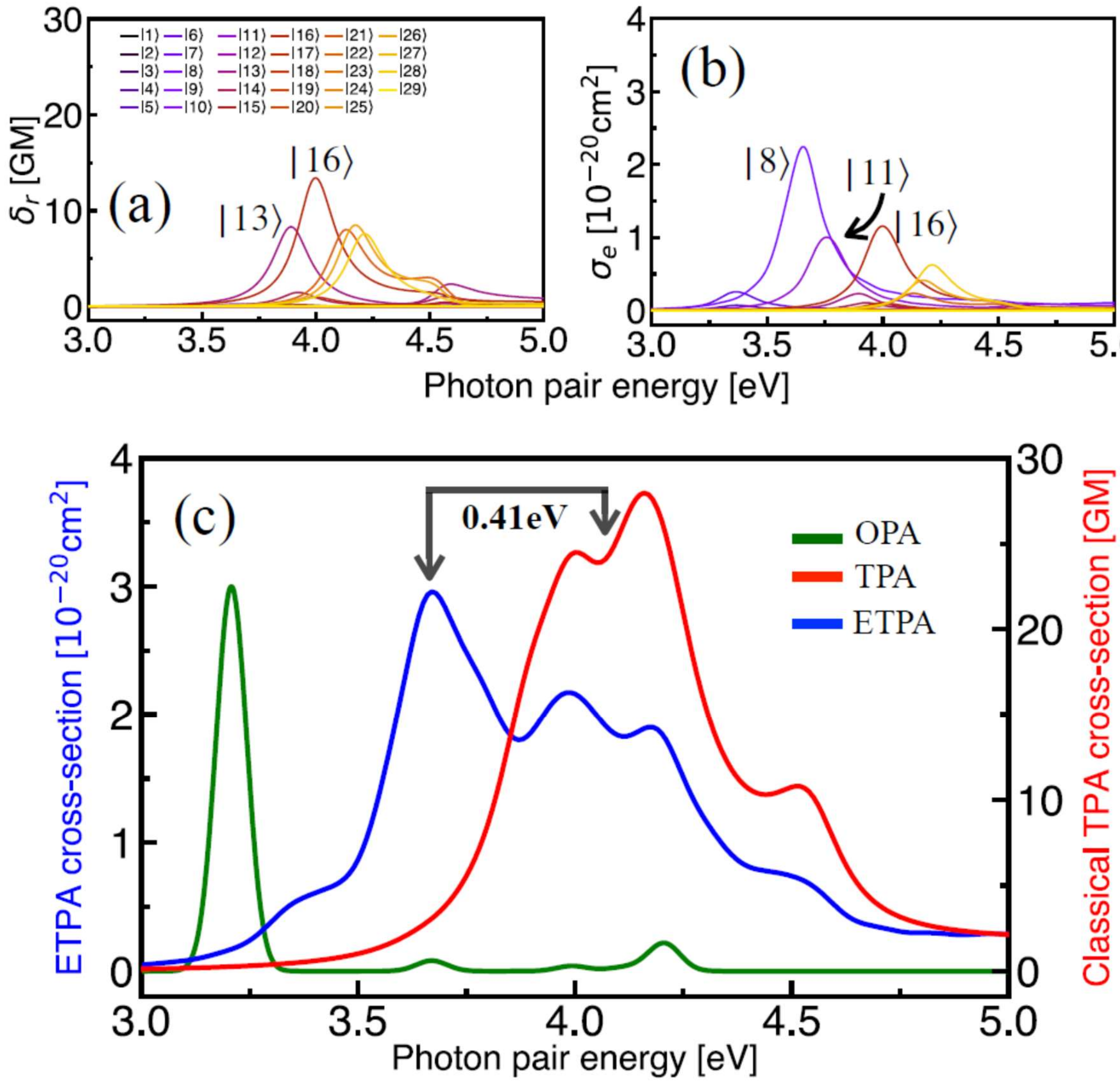
(a)
|13⟩
|16⟩
δ_r [GM]
(b)
|8⟩
|11⟩
|16⟩
σ_e [10^{-20}cm^2]
Photon pair energy [eV]
(c)
0.41eV
OPA
TPA
ETPA
ETPA cross-section [10^{-20}cm^2]
Classical TPA cross-section [GM]
Photon pair energy [eV]

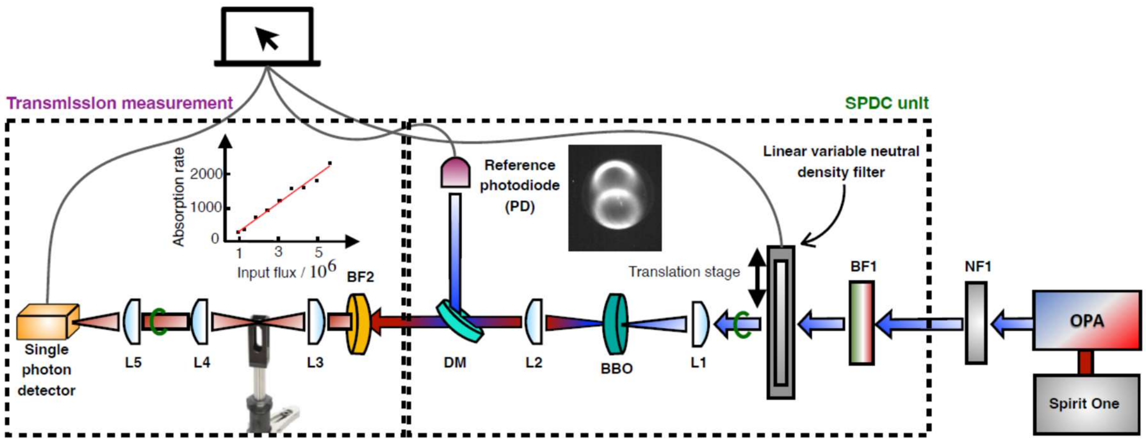
Transmission measurement
SPDC unit
Absorption rate
2000
1000
0
1
3
5
Input flux / 10^6
BF2
Reference
photodiode
(PD)
Linear variable neutral
density filter
Translation stage
BF1
NF1
OPA
Spirit One
Single
photon
detector
L5
L4
L3
DM
L2
BBO
L1